Identification of specific posttranslational *O*-mycoloylations mediating protein targeting to the mycomembrane

Clément Carel[a,1], Julien Marcoux[a,1], Valérie Réat[a], Julien Parra[a], Guillaume Latgé[a], Françoise Laval[a], Pascal Demange[a], Odile Burlet-Schiltz[a], Alain Milon[a], Mamadou Daffé[a], Maryelle G. Tropis[a], and Marie A. M. Renault[a,2]

[a]Institut de Pharmacologie et de Biologie Structurale, Université de Toulouse, CNRS, Université Paul Sabatier, 31000 Toulouse, France

Edited by William R. Jacobs Jr., Albert Einstein College of Medicine and Howard Hughes Medical Institute, Bronx, NY, and approved March 9, 2017 (received for review October 28, 2016)

The outer membranes (OMs) of members of the Corynebacteriales bacterial order, also called mycomembranes, harbor mycolic acids and unusual outer membrane proteins (OMPs), including those with α-helical structure. The signals that allow precursors of such proteins to be targeted to the mycomembrane remain uncharacterized. We report here the molecular features responsible for OMP targeting to the mycomembrane of *Corynebacterium glutamicum*, a nonpathogenic member of the Corynebacteriales order. To better understand the mechanisms by which OMP precursors were sorted in *C. glutamicum*, we first investigated the partitioning of endogenous and recombinant PorA, PorH, PorB, and PorC between bacterial compartments and showed that they were both imported into the mycomembrane and secreted into the extracellular medium. A detailed investigation of cell extracts and purified proteins by top-down MS, NMR spectroscopy, and site-directed mutagenesis revealed specific and well-conserved posttranslational modifications (PTMs), including *O*-mycoloylation, pyroglutamylation, and *N*-formylation, for mycomembrane-associated and -secreted OMPs. PTM site sequence analysis from *C. glutamicum* OMP and other *O*-acylated proteins in bacteria and eukaryotes revealed specific patterns. Furthermore, we found that such modifications were essential for targeting to the mycomembrane and sufficient for OMP assembly into mycolic acid-containing lipid bilayers. Collectively, it seems that these PTMs have evolved in the Corynebacteriales order and beyond to guide membrane proteins toward a specific cell compartment.

Corynebacteriales | *O*-acylation | sequence motif | top-down proteomics | NMR

Protein lipidation, once assumed to act as a stable membrane anchor for soluble proteins, is now attracting widespread attention for its emerging role in diverse signaling pathways and regulatory mechanisms (1). Among the different classes of posttranslational protein fatty acid modifications, *O*-acylation is quite rare. Only a few examples have been reported, mostly in eukaryotes. For example, the *O*-octanoylation of ghrelin, a secreted 28-aa peptide, is essential for growth hormone, orexigenic, metabolic, and insulin secretion effects (2, 3), whereas the *O*-palmitoleylation of Wingless (Wnt) signaling proteins is required for targeting to the endoplasmic reticulum and secretion and activation of cell surface receptors (4, 5). In contrast, *O*-mycoloylation recently discovered in Corynebacteriales (6) is the only type of *O*-acylation found in bacteria. This modification consists of the addition of a mycoloyl residue, a C32-C36 α-alkyl, β-hydroxy-fatty acyl chain, to serine residues through an *O*-ester linkage. *O*-mycoloylation is catalyzed by a well-conserved mycoloyltransferase C (cMytC), which was found to be associated with the bacterial cell envelope and secreted into the extracellular medium (7). cMytC belongs to the α/β hydrolase superfamily and uses trehalose dimycolate and protein as substrates.

Corynebacteriales, which are diderm Gram-positive bacteria, include species like *Corynebacterium glutamicum*, which has been harnessed for industrial production of amino acids, as well as *Corynebacterium diphtheriae* and *Mycobacterium tuberculosis*, which cause devastating human diseases. Corynebacteriales contain a unique structure termed the mycoloyl–arabinogalactan–peptidoglycan (mAGP) complex. The mAGP complex consists of a heteropolymer of peptidoglycan covalently linked to arabinogalactan, which in turn, is covalently associated with mycolic acids of the inner leaflet of the outer membrane. The collection of mycolic acids and associated membrane proteins is referred as the mycomembrane. To date, bacterial *O*-mycoloylation has been reported on small porins located in the cell envelope of *C. glutamicum* and homologs, including the cation-selective channels PorA (45 residues), PorH (57 residues), and protein of unknown function, ProtX, all of which are small polypeptides (6). Although the function and underlying mechanisms of *O*-mycoloylation remain elusive, the biological consequences of having long acyl moieties attached to proteins include enhancement of membrane binding as well as protein–protein interactions. For example, in vitro studies revealed that protein posttranslational modification (PTM) was essential for PorA/PorH pore-forming activity (8). Interestingly, the mycoloylated PorA, PorH, and ProtX proteins

Significance

Protein secretion is an essential determinant of bacterial physiology and virulence. Members of the Corynebacteriales order have evolved a complex cell envelope containing two membranes, a plasma membrane and an outer membrane, called the mycomembrane, which harbors mycolic acids and outer membrane proteins (OMPs) of unusual structure. Here, we have investigated the biogenesis of OMPs in *Corynebacterium glutamicum* and deciphered the role of *O*-mycoloylation in targeting OMPs to the mycomembrane. Partially enabled by our methodology, we found that the posttranslational state of major OMPs determined their presence in the outer membrane vs. the extracellular medium. We have also uncovered a short linear amino acid motif for *O*-acylation of proteins that seems to be preserved throughout the kingdoms.

Author contributions: C.C., J.M., P.D., O.B.-S., A.M., M.D., M.G.T., and M.A.M.R. designed research; C.C., J.M., V.R., J.P., G.L., F.L., and M.A.M.R. performed research; C.C., J.M., V.R., J.P., G.L., and M.A.M.R. contributed new reagents/analytic tools; C.C., J.M., V.R., J.P., G.L., F.L., P.D., O.B.-S., A.M., M.D., M.G.T., and M.A.M.R. analyzed data; and J.M., V.R., J.P., P.D., O.B.-S., A.M., M.D., M.G.T., and M.A.M.R. wrote the paper.

The authors declare no conflict of interest.

This article is a PNAS Direct Submission.

Data deposition: The data reported in this paper have been deposited in the Mass Spectrometry Interactive Virtual Environment (MassIVE) database, which is a community resource developed by the NIH-funded Center for Computational Mass Spectrometry to promote the global free exchange of MS data (dataset identifier MSV000080529; massive.ucsd.edu).

[1]C.C. and J.M. contributed equally to this work.

[2]To whom correspondence should be addressed. Email: marie.renault@ipbs.fr.

This article contains supporting information online at www.pnas.org/lookup/suppl/doi:10.1073/pnas.1617888114/-/DCSupplemental.

all lack dedicated signal sequences for export but are only found in the mycomembrane. Hence, it can be assumed that posttranslational *O*-mycoloylation may provide a structural element for subcellular targeting of secreted outer membrane proteins (OMPs).

Thus far, studies have failed to identify a well-defined sequence in mycomembrane-associated proteins that can function as a targeting signal. To decipher the putative role of *O*-mycoloylation in the biogenesis of mycomembrane-associated proteins, we used a strategy based on homologous expression and structural characterization of the four major porins in *C. glutamicum*, all of which are found or thought to be found in the mycomembrane. This set includes the cation-selective channels PorA and PorH, which do not contain any leader sequence and are posttranslationally modified by a mycolic acid on serine residues S15 and S56 (6, 9), respectively. In addition, we selected the anion-selective channel PorB and its homolog PorC containing 99 and 97 residues, respectively, after proteolytic cleavage of the N-terminal signal sequence specific for the Sec apparatus. The α-helical PorB (10) is known to be targeted to the cell wall, whereas PorC, by virtue of its colocation in the same operon, is thought to be similarly targeted, although no evidence currently exists for this (11). We first investigated the partitioning of endogenous or recombinantly expressed PorA, PorH, PorB, and PorC porins between bacterial compartments. Next, we purified proteins from each cell compartment and identified proteoforms containing PTMs that are associated with specific cellular compartments. We determined the nature and the position of the PTMs by combining site-directed mutagenesis, top-down electrospray ionization (ESI)-MS/MS, and NMR spectroscopy and propose short linear motifs for *O*-acylation of proteins from different kingdoms. Finally, we showed that the presence of one or multiple mycoloyl residue(s) constitutes the main driving force for membrane association and is essential for targeting porins to the mycolic acid-containing lipid bilayer.

Results

***C. glutamicum* Porins Are Targeted to the mAGP Complex and Secreted into the Extracellular Medium.** We first created recombinant expression systems for *C. glutamicum* porins in the native host and compared the distribution of His-tagged PorA, PorH, PorB, and PorC within the bacterial compartments. These experiments were carried out in both exponential and stationary growth phases of WT *C. glutamicum* (ATCC13032) expressing individual *porA*, *porH*, *porB*, and *porC* genes with native signal sequences using an isopropyl-β-D-1-thiogalactopyranoside (IPTG)-inducible Ptac promoter on high-copy plasmids (Table S1). After cell fractionation, the cytosol (CYT), the plasma membrane (PM), the mAGP comprising the mycomembrane-associated components, and the extracellular medium containing secreted proteins were isolated. Pure PM and mAGP fractions were obtained by sucrose density ultracentrifugation using a procedure described elsewhere (12). Cell debris was removed from CYT and extracellular medium fractions by two cycles of ultracentrifugation. SDS/PAGE followed by Western blot analysis of subcellular CYT, PM, and mAGP fractions showed that PorA, PorH, and PorB were correctly and specifically targeted to the outer membrane, and no residual signal was observed in other cell compartments (Fig. 1*A*). PorC was also found associated with the mAGP, constituting evidence for its specific targeting. Surprisingly, significant amounts of PorH, PorB, and PorC and traces of PorA were also detected in the extracellular medium, indicating the existence of soluble proteoforms secreted by the bacteria (Fig. 1*A*).

Posttranslational *O*-Acylation Is a Common Feature of Mycomembrane-Associated Porins, Whereas Secreted Porins Are Not Modified. Next, we wanted to test whether mAGP-associated PorA, PorH, PorB, and PorC proteins possess specific targeting and sorting signals that were absent in the secreted proteoforms. In this context, we carried out top-down nanoliquid chromatography (nano–LC)-MS

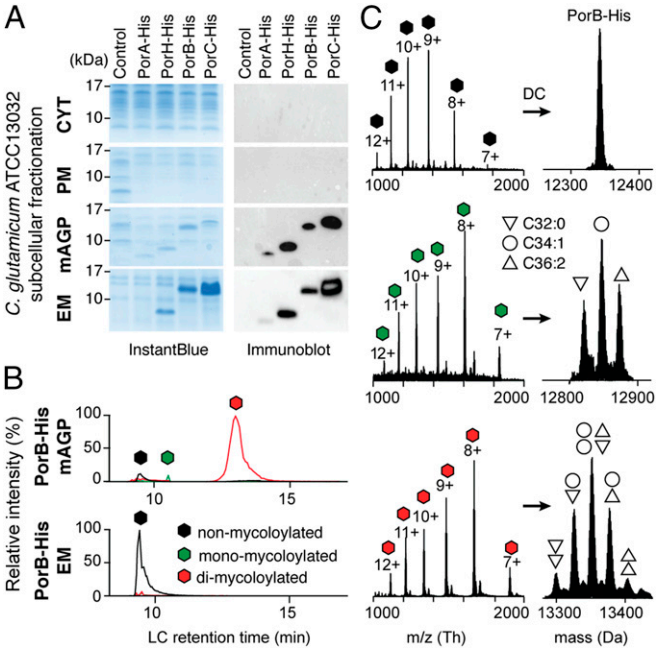

Fig. 1. Identification of distinct proteoforms for *C. glutamicum* OMPs associated with the mAGP complex and secreted in the extracellular medium. (*A*) *C. glutamicum* ATCC13032 cells expressing recombinant PorA-His, PorH-His, PorB-His, and PorC-His were cultured under identical conditions. Subcellular fractions corresponding to the CYT, the PM, the mAGP complex, and the extracellular medium were analyzed by SDS/PAGE after staining with InstantBlue (*Left*) and Western blotting (*Right*) with antibodies against the protein His tag. Fractions isolated from WT, untransformed cells were coanalyzed as control. Molecular mass markers (in kilodaltons) are indicated next to the gel. (*B*) Extracted ion chromatograms of PorB-His purified from mAGP (*Upper*) and extracellular medium (*Lower*) fractions containing nonmycoloylated (black), monomycoloylated (green), and dimycoloylated (red) proteoforms. (*C*) Representation of the multicharged MS spectra (*Left*) and deconvoluted (DC) spectra obtained for PorB-His proteoforms with isotopic resolution (*Right*). The mycolic acid compositions of each proteoform are indicated by triangle and circle symbols. EM, extracellular medium.

analysis on the recombinant porins purified from the extracellular medium (extracellular medium fraction) and the mAGP complex. We were able to separate the different proteoforms of both secreted and mAGP-associated porins using reverse-phase C4 chromatography (Fig. 1*B*), thus enabling subsequent detection and characterization by MS (Fig. 1*C*). The analysis of purified mAGP-associated PorB yielded three resolved chromatographic peaks (Fig. 1*B*, *Upper*) and high-quality MS spectra from multicharged species (Fig. 1*C*, *Left*). Because of the high resolution and mass accuracy of the MS instrumentation, the molecular weight determination of each proteoform was sufficient to unambiguously decipher the protein PTM. The first chromatographic peak (elution time of 9 min) corresponded to a mature, unmodified form of PorB (Fig. 1*C*, *Top*), whereas the second peak (elution time of 10.5 min) contained three proteoforms with mass increments of 478.5, 504.6, and 530.6 Da that could readily be assigned as monoacylated species with C32:0, C34:1, and C36:2 mycolic acyl residues, respectively (Fig. 1*C*, *Middle*). The third chromatographic peak (elution time of 13.5 min) consisted of dimycoloylated proteoforms with five distinct acylation patterns: C32:0/C32:0, C34:1/C32:0, C34:1/C34:1 or C32:0/C36:2, C34:1/C36:2, and C36:2/C36:2 (Fig. 1*C*, *Bottom*), reflecting the mycolic acid composition of the *C. glutamicum* mycomembrane under standard bacterial growth conditions (6). Overall, nine distinct proteoforms of PorB were found to be associated with the mAGP complex compartment. Assuming that the ionization yields of the mycoloylated and nonmycoloylated

species were roughly similar, we could compare the signal intensities of a given charge state (9+) obtained for each species, showing a significant prevalence of dimycoloylated PorB species in the mAGP complex (Figs. 1*B* and 2*C*, *Top*). Next, we performed the analysis of secreted PorB under identical experimental conditions (Fig. 1*B*, *Lower*) and found a single proteoform that was consistent with mature, nonacylated PorB (Fig. 1*C*, *Top*). These results prompted us to extend the analysis to other recombinant porins and check whether the *O*-acylation represented the major structural discrepancy between secreted and mAGP-associated porins. Following identical protocols, we found that PorA, PorH, and PorC purified from the extracellular medium were all consistent with nonmycoloylated species, whereas mAGP-associated proteoforms were acylated by one or two mycolic acids (Fig. S1). Together, these results confirmed that posttranslational *O*-acylation is a common feature of mAGP-associated porins, whereas secreted proteins are not acylated (Table S2). We show that (*i*) PorB and PorC have been shown to be mycoloylated, (*ii*) polymycoloylation is evidenced at the molecular level, and (*iii*) any of four porins have been found in a secreted, soluble form.

The Secretion of Nonacylated Porins Is Physiologically Relevant. Whereas *O*-mycoloylated porins have been previously identified from natural extracts of *C. glutamicum* and other Corynebacteriales (6), the detection of soluble proteoforms in the extracellular medium has remained elusive. In this context, we wanted to further investigate the modifications on secreted proteoforms using top-down nano–LC-MS/MS. Although collision-induced dissociation (CID) fragmentation may prevent the detection of most labile modifications, such as phosphorylation and *O*-glycosylation, it generally yields better fragmentation. In the case of *O*-mycoloylation, we did not see any neutral loss of the mycolic acid residue, allowing their precise localization. All of the proteoforms of PorA-His and PorH-His were systematically found with a mass increment of +28 Da that was readily assigned to the formylation of the N-terminal methionine. Interestingly, secreted PorA-His was alternatively found with an additional mass difference of +80 Da, consistent with the phosphorylation of a hydroxyl residue in addition to the N-terminal formylation (Fig. S1). However, this phosphorylation was further localized on the S51, which is part of the additional residues of the His-Tag (Table S2). PorC proteoforms were characterized by a mass discrepancy of −19 Da, in agreement with the presence of a disulfide bond (−2 Da) and the cyclization of the N-terminal glutamyl residue on signal peptide cleavage, yielding a pyroglutamyl residue (−17 Da) (Table S2). Although such N-terminal protein modifications (i.e., *N*-formylation and the formation of pyroglutamyl residues) have been identified in bacterial secreted proteins and OMPs (13, 14), we sought additional evidence about the natural relevance of secreted porin species. To check whether nonacylated soluble porins resulted from a physiological secretion process, endogenous proteins secreted from stationary-phase, untransformed *C. glutamicum* cells were isolated using an identical protocol. We then conducted a discovery mode data-dependent analysis, in which the three most intense precursors of each MS scan were selected and fragmented. The resulting MS/MS spectra were then automatically searched against the *C. glutamicum* protein database in discovery mode (*SI Experimental Procedures*). This unbiased approach enabled the identification of 24 proteins in WT *C. glutamicum*, among which the nonacylated PorB, PorH, and PorA were unambiguously identified with good mass accuracy (<20 ppm) and sequence coverage (30–50% of the fragments explained) (Fig. S2), thus confirming that secretion of nonacylated porins is physiologically relevant. Furthermore, the *N*-formylation of PorA and PorH together with PorB disulfide bridge formation were also confirmed. We found identical proteoforms at the same retention times for PorB, PorH, and PorA in the extracellular medium extract of the *C. glutamicum* ΔcMytC strain for which the cMytC responsible for the *O*-acylation of mAGP-associated PorA and PorH porins has been deleted. However, in contrast to recombinantly expressed PorC, endogenous protein was not detected in the extracellular medium. This result suggests that PorC is not readily expressed by the bacterium under standard in vitro conditions, consistent with a previous publication (11).

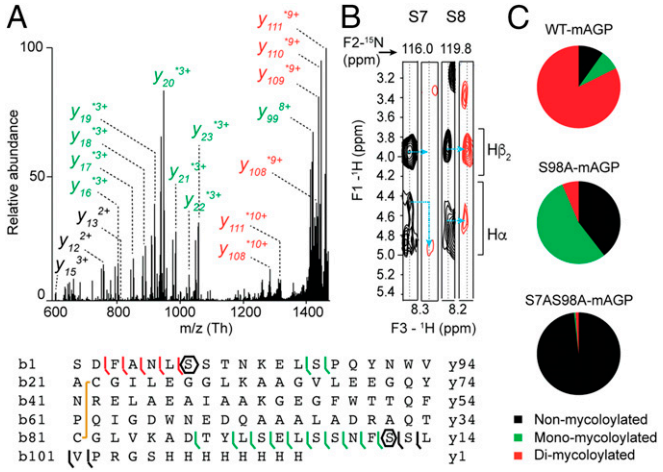

Fig. 2. Characterization of protein modifications by MS/MS, NMR, and site-directed mutagenesis. Example of PorB. (*A*) Top-down CID of dimycoloylated PorB-His-10+ charge state (*m/z* 1,336.10 Th) with nonmycoloylated, monomycoloylated, and dimycoloylated *y* and *b* fragments colored black, green, and red, respectively. The sequence coverage was obtained by fragmenting the 8+, 9+, and 10+ charge states of PorB-His, identifying S98 and S7/S8 residues (polygons) as putative mycoloylation sites and a disulfide bond between C22 and C81 (yellow line). (*B*) Solution NMR analysis of nonmycoloylated (black) and mycoloylated (red) PorB-His. Selected strips extracted from 3D ^{1}H, ^{15}N, ^{1}H heteronuclear single quantum coherence–total correlation spectroscopy (HSQC-TOCSY) spectra obtained on (U-^{15}N)–labeled PorB-His showing Hα and Hβ$_2$ chemical shifts of S7 and S8 residues for the two proteoforms. Although ^{1}H resonances from S8 were not affected, significant spectral changes were observed for Hα of residue S7 (blue arrows), thus identifying the *O*-acylation of the S7 hydroxyl of PorB-His. (*C*) The positions of PTM within the protein sequence were validated by site-directed mutagenesis of S7 and S98 residues and subsequent MS analysis of PorB-His WT (WT-mAGP; *Top*) and its mutant derivatives PorB-S98A (S98A-mAGP; *Middle*) and PorB-S7AS98A (S7AS98A-mAGP; *Bottom*). Nonmycoloylated (black), monomycoloylated (green), and dimycoloylated (red) proteoforms were semiquantified from extracted ion chromatograms of the corresponding 9+ charge states.

Identification of *O*-Acylation Sites by Combining MS/MS, NMR, and Site-Directed Mutagenesis. Previously, we have shown that PorA and PorH were *O*-mycoloylated on S15 (6) and S56 residues (9), respectively. The identification of *O*-acylation sites within mono- and multiacylated proteoforms of PorB and PorC represents a new challenge considering the protein size, the large number of acylated proteoforms, and the putative heterogeneity of *O*-mycoloylation sites. As shown in Fig. 2*A*, CID fragmentation of PorB dimycoloylated proteoforms yielded a set of unmodified, monomycoloylated, and dimycoloylated fragment ions consistent with the presence of a first *O*-acylation site on S98 and a second site located between S7-L13. The analysis of fragment ions stemming from monomycoloylated PorB proteoforms confirmed these results but did not allow determining whether S7 or S8 was the site of modification (Fig. S3*A*). To decipher the position of the *O*-acylation within this protein segment, we analyzed and compared the ^{1}H sidechain chemical shifts of serine residues S7 and S8 in nonacylated and acylated (U-^{15}N)–labeled PorB (Fig. 2*B*). As expected, well-defined ^{1}H resonances were observed at expected chemical shifts for both S7 and S8 residues of the nonacylated PorB sample [Fig. 2*B* (note that the Hα resonance of S8 is obscured by overlap with the peak from the Hα of

residue F3) and Fig. S4]. However, both Hα and Hβ resonances of residue S7 exhibited significant differences between nonacylated and acylated PorB species. In particular, the Hα chemical shift of S7 was strongly perturbed by acylation and shifted from 4.45 to a different frequency, likely at 4.90 ppm. The Hβ resonance was broadened beyond detection, probably because of the presence of conformational exchange in the millisecond range. However, the S8 ^{1}H resonances of acylated PorB were not affected, thus suggesting the S7 hydroxyl group as the sole site of *O*-acylation within the protein segment S7-L13. To confirm the *O*-acylation sites, we generated a set of single and double mutants in which the native serine was substituted by an alanine (i.e., PorB-S98A, PorB-S7A, and PorB-S7AS98A). We purified both secreted and mAGP-associated PorB mutants and confirmed the presence of the mutations and a concomitant loss of PTM in a semiquantitative manner (Fig. 2*C* and Fig. S5*A*). This strategy was also successfully applied to the mono and dimycoloylated proteoforms of PorC, leading to the unambiguous identification of acylation sites on residues S87 and S91 (Figs. S3 *B* and *C* and S5*B*).

Sequence Analysis of PTM Sites Reveals Consensus Patterns for *O*-Acylation. After complete PTM mapping of secreted and mAGP-associated *C. glutamicum* porins PorA, PorH, PorB, and PorC had been obtained (Fig. 3*A* and Table S2), we examined the amino acid composition of the *O*-acylation sites. The data were analyzed using the Motif-X algorithm, but no specific motif was found, indicating that the conservation is not strong (15). Therefore, we constructed an alignment of known *O*-acylated peptides comprising *C. glutamicum* porins and human Ghrelin and Wnt-3a (Fig. 3*B*), centered on the modified serine residue, that revealed moderately conserved short linear motifs around the PTM site. The frequency of residue- and position-specific amino acid occurrences was calculated. These *O*-acylation sites exhibited an increased occurrence of certain amino acids (e.g., S, L, N, and F) and the total absence of others (R, M, W, and Y) for both *C. glutamicum* and human proteins. The enrichment factor depended on the proximity to the modified serine, suggesting a putative role of these residues in enzyme–substrate interactions. Subsequently, we examined if such short linear amino acid stretches were conserved among PorA, PorH, PorB, and PorC orthologs (Fig. S6). Each query sequence was searched using BLAST against the Corynebacteriales proteome, and only sequences having at least 30% global similarity to the original query were kept for inclusion. Orthology was detected in more than 10 different organisms, including *C. diphtheria* and *Corynebacterium efficiens*, species known to possess mycoloyltransferase activity or mycoloylated proteins associated with the cell envelope (6, 7). We found that the motif was well-conserved between orthologs in contrast to generally nonconserved surrounding regions of the protein. Focusing on regions with evolutionarily conserved residues, we discovered putative *O*-acylation sites within cell envelope-associated proteins in *C. glutamicum*, such as lipocalin, flotillin, esterase, and mycoloyltransferase (Table S3). These proteins are known to interact with the outer membrane in their nonacylated (mycoloyltransferase and esterase) or acylated (lipocalin and flotillin) forms in Corynebacteriales and Gram-negative bacteria. These results strongly suggest the presence of short linear motifs that can be *O*-acylated and in the case of *C. glutamicum* proteins, result in mAGP association. These sequences may have been evolutionarily conserved across kingdoms, because they have also been detected in two human *O*-acylated proteins.

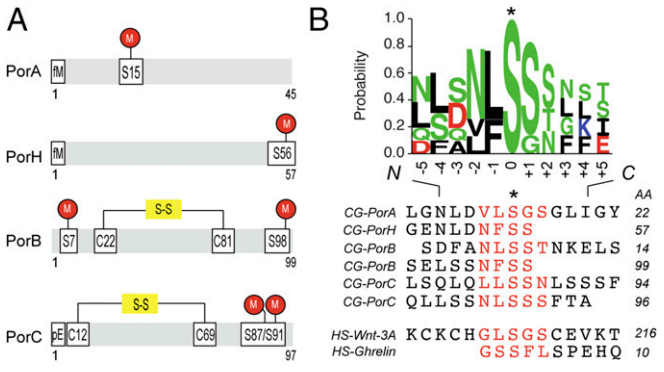

Fig. 3. *O*-acylation of OMPs occurs in short linear motifs. (*A*) Schematic representation of protein modifications along the protein sequences of *C. glutamicum* PorA, PorH, PorB, and PorC. The sites of modifications are reported onto the sequence using the following code: M, *O*-mycoloylation; pE, pyroglutamate; and S-S, disulfide bond. (*B*) Sequence alignments of selected *O*-acylated proteins from *C. glutamicum* and human genomes within a region surrounding the fatty acylation residue. The sequence logo was calculated from the *C. glutamicum* peptide sequences only and displays the position-specific frequency of each amino acid composing the motif. AA, amino acid; *CG*, *C. glutamicum*; *HS*, *Homo sapiens*. *Fatty acylation residue.

Targeting to the mAGP Complex Is Dependent on the Presence of the *O*-Mycoloylation. Protein acylation often regulates trafficking, segregation, or clustering of proteins within membrane compartments (16). To ascertain that the *O*-mycoloylation plays a role in protein targeting to the mycomembrane, we expressed PorA, PorH, PorB, and PorC in WT and *cmytC*-deleted *C. glutamicum* strains using an IPTG-inducible Ptac promoter on a high-copy plasmid (pXmj19) and compared the distribution of recombinant porins within the mAGP complex and the PM (Fig. 4*A*). Results showed the absence of nonacylated mature His-tagged PorH, PorB, and PorC in both the mAGP complex and the PM when cMytC is depleted, confirming that *O*-acylation plays an essential role in the targeting and/or the retention of proteins to the mycomembrane. However, a significant amount of PorA was detected in the mycomembrane and to a lesser extent, the PM when *O*-mycoloylation activity was abolished. The PorA sequence clearly contains a stretch of 45 predominantly hydrophobic residues that is not present in the other porins. This inherent hydrophobicity likely explains the residual membrane association of the unmodified protein. Interestingly, the loss of the mycoloyl residue was associated with a nonspecific membrane association with both the mAGP complex and the PM. Furthermore, because multiacylated proteoforms were characterized for both PorB and PorC, we questioned whether both PTMs were mandatory for mAGP localization (Fig. 4*B*). Consequently, we monitored the presence of WT PorB and PorC and mutant derivatives PorB-S7A, PorB-S98A, PorB-S7AS98A, PorC-S87A, PorC-S91A, and PorC-S87AS91A in mAGP fractions when expressed in the WT *C. glutamicum* strain. Although mature forms of PorB and PorC were predominantly found associated with the mAGP fraction, aggregated forms of nonacylated precursor were copurified in the case of PorC (Fig. S7). As depicted in Fig. 4*B*, mutation of the S7 site of PorB and S91 site of PorC significantly reduced the association of these proteins with mAGP complex. In contrast, mutation of S98 in PorB and S87 in PorC resulted in minimal or no change in mAGP association, suggesting that, in both proteins, association is driven by predominantly one mycoloylation site (i.e., PorB-S7 and PorC-S91). Dual mutants of these proteins totally abrogated mAGP association and in both cases, result in enhanced secretion of nonacylated PorB and PorC into the extracellular medium.

Discussion

Protein secretion is an essential determinant of bacterial physiology and virulence, and a variety of mechanisms are responsible for transporting proteins into or across the PM, maintaining them in a soluble form, targeting them to their correct cell envelope locations,

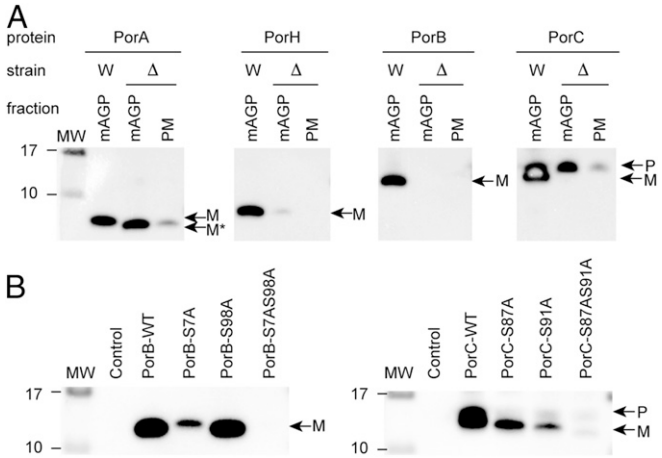

Fig. 4. The *O*-acylation is essential for retention of PorH, PorB, and PorC at the mycomembrane but not PorA. (*A*) The mAGP complex and the PM were isolated from WT (W) and cMytC-deficient (Δ) *C. glutamicum* strains expressing recombinant PorA-His, PorH-His, PorB-His, and PorC-His and analyzed by SDS/PAGE after immunodecoration with antibodies against protein His tag. (*B*) Analysis of the mAGP complex purified from WT *C. glutamicum* cells expressing native recombinant proteins (WT) or the mutant derivatives of PorB-His [i.e., PorB-S7A, PorB-S98A, and PorB-S7AS98A (*Left*)] and PorC-His [i.e., PorC-S87A, PorC-S91A, and PorC-S87AS91A (*Right*)] by SDS/PAGE and immunodecoration with antibodies against protein His tag. Fractions isolated from untransformed WT cells were coanalyzed as control. Bands corresponding to the recombinant proteoforms are indicated with arrows using the following code: M, mature form corresponding to the recombinant protein without its N-terminal signal sequence; M*, mature form without *O*-mycoloylation; P, recombinant protein precursor containing the N-terminal signal sequence. Molecular mass (MW) markers (in kilodaltons) are indicated next to the gel.

and then, folding them into the correct structures. Corynebacteriales have evolved a complex cell envelope containing a PM and a mycomembrane harboring mycolic acids and unusual OMPs. Additionally, an outermost layer may exist in some suborder (17, 18). The biogenesis and the organization of the Corynebacteriales mycomembrane are far less documented than for the LPS-containing counterpart from Gram-negative outer membranes (19–21). Notably, very few mycomembrane proteins have been structurally and functionally characterized (10, 22), and secretion pathways resulting in mycomembrane association remained an enigma.

In this paper, we investigated the biogenesis of OMPs in *C. glutamicum* and deciphered the role of *O*-mycoloylation in targeting OMPs to the mycomembrane by using dedicated expression systems, refined cell fractionation procedures, and a combination of NMR and advanced top-down MS approaches (Fig. 5). In contrast to traditional bottom-up proteomics relying on trypsin digestion, the top-down MS approach consists of the analysis of entire proteins, enabling the identification of combinations of PTMs and the direct semiquantification of proteoforms (23–25). This approach is particularly relevant for the analysis of *C. glutamicum* porins that are rather hydrophobic with the presence of PTMs consisting of C32-C36 mycoloyl residues and that lack arginine and lysine residues for the generation of adequate tryptic peptides. This strategy was developed on both purified recombinant proteins and crude cell extracts and yielded the unambiguous identification of nonacylated, monoacylated, and diacylated proteoforms. Each proteoform was then analyzed and fragmented individually to determine the nature and the position of the PTM sites. In total, we identified 5 proteoforms for PorA (with an *N*-formylation on M1 associated or not with a phosphorylation on S51 or a mycoloylation of S15), 4 proteoforms for PorH (with an *N*-formylation on M1 associated or not with a mycoloylation of S56), 9 proteoforms for PorC (with a disulfide bond and a pyroglutamylation that are associated or not with one or two mycoloyl residues on S87 and S91), and 12 proteoforms for PorB (with a disulfide bond associated or not with one or two mycoloyl residues on S7 and S98).

The analysis of the *O*-mycoloylation sites reveals conserved short linear motifs, which typically consist of a three- to four-residue stretch of the protein sequence with one or two more wildcard positions [i.e., (F/L)SS and VLSG]. Multiple sequence alignments showed a good conservation of the PTM site composition and localization within the orthologous protein sequences (Fig. S6). More importantly, we identified the *O*-acylation motif in a larger panel of *C. glutamicum* proteins involved in the biogenesis of the cell envelope, including mycoloyltransferases, an acyl transferase, and a peptidoglycan hydrolase, or the maintenance of its integrity, such as lipocalin and flotillin. Whereas the two latter proteins are known to be acylated in *Escherichia coli* via an amide linkage (26–29), other proteins, including the mycoloyltransferases, have only been characterized in their soluble, nonacylated forms (7, 30, 31). Furthermore, we showed a physicochemical similarity in the properties of the *O*-acylation sites between Corynebacteriales and two human proteins (i.e., the ghrelin and Wnt-3a). This observation suggests a possible similarity in the recognition of these sites by the acylating enzymes. In eukaryotes, posttranslational *O*-acylation is carried out by dedicated membrane-bound *O*-acyl transferases (MBOATs). Porcupine, the Wnt MBOAT, appends palmitoleate and shorter *cis*-unsaturated fatty acids to Wnt. A consensus sequence in Wnt-3a (CXCHGXSXXCXXKXC) surrounding the acylated S209 mediates enzyme binding, fatty acid transfer, and Wnt signaling with G207, K215, and disulfide bonds required for fatty acylation (32). In ghrelin, the octanoate is linked to S3 within the N-terminal GSSFL sequence, with G1 and F4 also

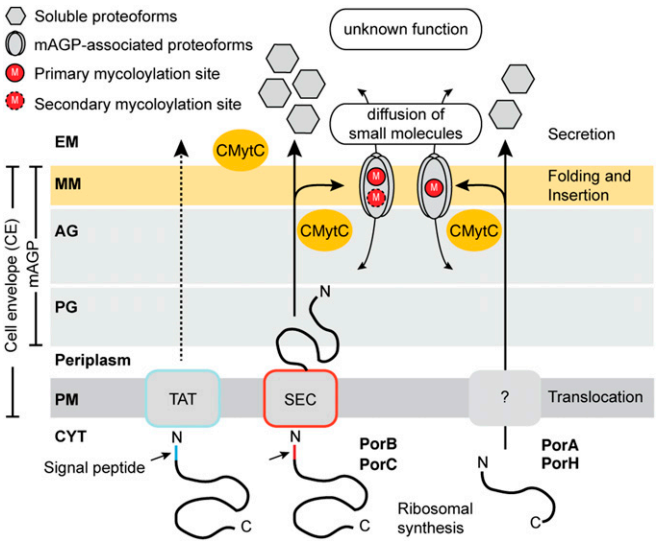

Fig. 5. Model for the biogenesis of major OMPs in *C. glutamicum*. After synthesis in the CYT and translocation across the PM through Sec-dependent (PorB and PorC) or –independent (PorA and PorH) pathways, OMPs are transported into the periplasm and acylated with one or several mycolic acids by the cMytC on serine residues located within short linear motifs. Specific posttranslational *O*-mycoloylations of OMPs are essential for targeting to the mycomembrane and may be involved in the subsequent formation of pore-forming assemblies. Nonacylated proteoforms are released in the extracellular medium (EM), but their function remains to be elucidated. AG, arabinogalactan; PG, peptidoglycan; M, *O*-mycoloylation; MM, mycomembrane; PM, plasma membrane; SEC, general secretion pathway; TAT, twin arginine translocation pathway.

contributing to substrate recognition by Ghrelin *O*-acyltransferase (3, 33).

We showed that the mycoloyl residue is a bona fide signal to direct the modified protein to bind to mycomembrane (Fig. 4). There seems to be a correlation between the hydrophilicity and the amount of mycoloylation (Fig. 4*B*). Thus, PorB and PorC being the most hydrophilic porins are predominantly doubly mycoloylated. When protein *O*-acylation is abolished in the bacterium, PorB, PorC, and PorH are released into the extracellular medium, implying that mycolate hydrophobicity is the main driving force for mycomembrane association. However, for PorA, which is much more hydrophobic, a substantial amount of nonacylated protein remained associated with the membranes. Interestingly, PorA is not specifically associated with the mycomembrane when nonmycoloylated, and it is also detected in the PM (Fig. 4*A*), confirming the essential role of the mycoloylation for specific targeting to the mAGP complex.

The *O*-ester linkage between a mycoloyl residue and the protein is relatively stable. So far, an esterase/hydrolase activity that could cleave a mycoloyl residue from serine has not been shown. However, the existence of nonacylated soluble proteoforms might suggest the reversibility of the *O*-mycoloylation and resulting porin trafficking between the (myco)membrane and the extracellular medium. Indeed, we showed that nonacylated PorB, PorC, and PorH were predominantly secreted (Figs. 1 and 4 and Fig. S1). Hence, like Wnt proteins, for which palmitoleylation was recently shown to be reversible (34, 35), fatty acid cleavage by a carboxylesterase may regulate targeting of hydrophilic porins. Indeed, such potential carboxylesterases/hydrolases with a consensus mycoloylation site have been found in *C. glutamicum* (Table S3). This study has advanced our understanding of membrane biogenesis in Corynebacteriales. Nonetheless, important questions remain. One crucial issue is determining whether the *O*-mycoloylation is a general process to specifically retain proteins at the mycomembrane in *C. glutamicum* and other Corynebacteriales or indeed, if it is the only modification capable of doing so. Of equal importance will be determining the molecular mechanisms by which *O*-acylation affects OMP folding and interaction with the mycomembrane. This research line will generate knowledge in fundamental microbiology and in so doing, could bring to light vulnerabilities that could be exploited for new antibacterial drugs or provide efficient new industrial biotechnology procedures.

Experimental Procedures

Expression of Recombinant Cg Porins. Plasmid construction, site-directed mutagenesis, and bacterial growth media are described in *SI Experimental Procedures*. For the expression of C-terminal His-tag fusion proteins, Brain Hearth Infusion or CGXII growth medium was inoculated with freshly transformed *C. glutamicum* cells at A_{600} of 0.4. The expression of LacI-regulated genes was induced by adding 1 mM IPTG in the early log phase (i.e., $A_{600} \sim 3$–4) and maintained during 16–18 h at 30 °C. Cell fractionation and protein purification were achieved using procedures described in *SI Experimental Procedures*.

Top-Down LC-MS and LC-MS/MS. Nano–LC-MS and MS/MS analyses of cell extracts (extracellular medium fractions) and purified recombinant proteins were performed on a nanoRS UHPLC system (Dionex) coupled to an LTQ-Orbitrap Velos mass spectrometer (ThermoFisher Scientific). Additional information on experimental procedures is in *SI Experimental Procedures*. Data have been deposited in the Mass Spectrometry Interactive Virtual Environment repository with the dataset identifier MSV000080529 (massive.ucsd.edu).

ACKNOWLEDGMENTS. We thank Profs. M. Bott and R. Freudl for providing the empty pAN6 plasmid and Prof. R. Benz for providing pXmj19 plasmids with PorA and PorH genes. This work and the postdoctoral fellowship of C.C. were supported by French National Research Agency "Young Researcher" Grant ANR-13-JSV8-0001-01 (to M.A.M.R.). We acknowledge financial support from Integrated Screening Platform of Toulouse–Genotoul platform of Toulouse, CNRS, Université de Toulouse–Université Paul Sabatier, European Structural Funds (Fonds Européens de Développement Régional), the Midi-Pyrénées region, and Toulouse Metropole for the NMR and MS equipment.

1. Resh MD (2016) Fatty acylation of proteins: The long and the short of it. *Prog Lipid Res* 63:120–131.
2. Kojima M, et al. (1999) Ghrelin is a growth-hormone-releasing acylated peptide from stomach. *Nature* 402:656–660.
3. Gutierrez JA, et al. (2008) Ghrelin octanoylation mediated by an orphan lipid transferase. *Proc Natl Acad Sci USA* 105:6320–6325.
4. Takada R, et al. (2006) Monounsaturated fatty acid modification of Wnt protein: Its role in Wnt secretion. *Dev Cell* 11:791–801.
5. Nile AH, Hannoush RN (2016) Fatty acylation of Wnt proteins. *Nat Chem Biol* 12: 60–69.
6. Huc E, et al. (2010) O-mycoloylated proteins from Corynebacterium: An unprecedented post-translational modification in bacteria. *J Biol Chem* 285:21908–21912.
7. Huc E, et al. (2013) Identification of a mycoloyl transferase selectively involved in O-acylation of polypeptides in Corynebacteriales. *J Bacteriol* 195:4121–4128.
8. Rath P, et al. (2011) Functional expression of the PorAH channel from *Corynebacterium glutamicum* in cell-free expression systems: Implications for the role of the naturally occurring mycolic acid modification. *J Biol Chem* 286:32525–32532.
9. Rath P, et al. (2013) NMR localization of the O-mycoloylation on PorH, a channel forming peptide from Corynebacterium glutamicum. *FEBS Lett* 587:3687–3691.
10. Ziegler K, Benz R, Schulz GE (2008) A putative α-helical porin from *Corynebacterium glutamicum*. *J Mol Biol* 379:482–491.
11. Costa-Riu N, et al. (2003) Identification of an anion-specific channel in the cell wall of the Gram-positive bacterium *Corynebacterium glutamicum*. *Mol Microbiol* 50:1295–1308.
12. Marchand CH, et al. (2012) Biochemical disclosure of the mycolate outer membrane of *Corynebacterium glutamicum*. *J Bacteriol* 194:587–597.
13. Dalbøge H, Bayne S, Pedersen J (1990) *In vivo* processing of N-terminal methionine in *E. coli*. *FEBS Lett* 266:1–3.
14. Carrillo DR, et al. (2010) Kinetic and structural characterization of bacterial glutaminyl cyclases from *Zymomonas mobilis* and *Myxococcus xanthus*. *Biol Chem* 391:1419–1428.
15. Chou MF, Schwartz D (2011) Biological sequence motif discovery using motif-x. *Curr Protoc Bioinformatics* 13:13.15–13.24.
16. Sorek N, Bloch D, Yalovsky S (2009) Protein lipid modifications in signaling and subcellular targeting. *Curr Opin Plant Biol* 12:714–720.
17. Hoffmann C, Leis A, Niederweis M, Plitzko JM, Engelhardt H (2008) Disclosure of the mycobacterial outer membrane: Cryo-electron tomography and vitreous sections reveal the lipid bilayer structure. *Proc Natl Acad Sci USA* 105:3963–3967.
18. Zuber B, et al. (2008) Direct visualization of the outer membrane of mycobacteria and corynebacteria in their native state. *J Bacteriol* 190:5672–5680.
19. De Geyter J, et al. (2016) Protein folding in the cell envelope of *Escherichia coli*. *Nat Microbiol* 1:16107.
20. Freudl R (2013) Leaving home ain't easy: Protein export systems in Gram-positive bacteria. *Res Microbiol* 164:664–674.
21. van der Woude AD, Luirink J, Bitter W (2013) Getting across the cell envelope: Mycobacterial protein secretion. *Curr Top Microbiol Immunol* 374:109–134.
22. Niederweis M (2003) Mycobacterial porins–new channel proteins in unique outer membranes. *Mol Microbiol* 49:1167–1177.
23. Marcoux J, Cianférani S (2015) Towards integrative structural mass spectrometry: Benefits from hybrid approaches. *Methods* 89:4–12.
24. Tran JC, et al. (2011) Mapping intact protein isoforms in discovery mode using top-down proteomics. *Nature* 480:254–258.
25. Siuti N, Kelleher NL (2007) Decoding protein modifications using top-down mass spectrometry. *Nat Methods* 4:817–821.
26. Bishop RE, Penfold SS, Frost LS, Höltje JV, Weiner JH (1995) Stationary phase expression of a novel *Escherichia coli* outer membrane lipoprotein and its relationship with mammalian apolipoprotein D. Implications for the origin of lipocalins. *J Biol Chem* 270:23097–23103.
27. Flower DR, North AC, Sansom CE (2000) The lipocalin protein family: Structural and sequence overview. *Biochim Biophys Acta* 1482:9–24.
28. Neumann-Giesen C, et al. (2004) Membrane and raft association of reggie-1/flotillin-2: Role of myristoylation, palmitoylation and oligomerization and induction of filopodia by overexpression. *Biochem J* 378:509–518.
29. Barák I, Muchová K (2013) The role of lipid domains in bacterial cell processes. *Int J Mol Sci* 14:4050–4065.
30. Brand S, Niehaus K, Pühler A, Kalinowski J (2003) Identification and functional analysis of six mycolyltransferase genes of Corynebacterium glutamicum ATCC 13032: The genes cop1, cmt1, and cmt2 can replace each other in the synthesis of trehalose dicorynomycolate, a component of the mycolic acid layer of the cell envelope. *Arch Microbiol* 180:33–44.
31. De Sousa-D'Auria C, et al. (2003) New insights into the biogenesis of the cell envelope of corynebacteria: Identification and functional characterization of five new mycoloyltransferase genes in *Corynebacterium glutamicum*. *FEMS Microbiol Lett* 224:35–44.
32. Rios-Esteves J, Haugen B, Resh MD (2014) Identification of key residues and regions important for porcupine-mediated Wnt acylation. *J Biol Chem* 289:17009–17019.
33. Yang J, Brown MS, Liang G, Grishin NV, Goldstein JL (2008) Identification of the acyltransferase that octanoylates ghrelin, an appetite-stimulating peptide hormone. *Cell* 132:387–396.
34. Zhang X, et al. (2015) Notum is required for neural and head induction via Wnt deacylation, oxidation, and inactivation. *Dev Cell* 32:719–730.
35. Kakugawa S, et al. (2015) Notum deacylates Wnt proteins to suppress signalling activity. *Nature* 519:187–192.